


Article

In Situ Synchrotron X-ray Diffraction Reciprocal Space Mapping Measurements in the RF-MBE Growth of GaInN on GaN and InN

Tomohiro Yamaguchi ^{1,*} , Takuo Sasaki ², Seiji Fujikawa ², Masamitsu Takahashi ², Tsutomu Araki ³, Takeyoshi Onuma ¹, Tohru Honda ¹ and Yasushi Nanishi ³

¹ Department of Applied Physics, School of Advanced Engineering, Kogakuin University, Tokyo192-0015, Japan; onuma@cc.kogakuin.ac.jp (T.O.); ct11761@ns.kogakuin.ac.jp (T.H.)

² Synchrotron Radiation Research Center, National Institutes for Quantum and Radiological Science and Technology (QST), Hyogo 679-5148, Japan; sasaki.takuo@qst.go.jp (T.S.); fujikawa.seiji@qst.go.jp (S.F.); takahashi.masamitsu@qst.go.jp (M.T.)

³ Department of Electrical & Electronic Engineering, Ritsumeikan University, Kyoto 525-8577, Japan; tara@se.ritsumei.ac.jp (T.A.); nanishi@se.ritsumei.ac.jp (Y.N.)

* Correspondence: t-yamaguchi@cc.kogakuin.ac.jp; Tel.: +81-42-628-4651

Received: 31 October 2019; Accepted: 25 November 2019; Published: 28 November 2019



Abstract: In this work, in situ synchrotron X-ray diffraction reciprocal space mapping (RSM) measurements were carried out for the radio-frequency plasma-assisted molecular beam epitaxy (RF-MBE) growth of GaInN on GaN and InN layers, which were also grown by RF-MBE on commercialized GaN/*c*-sapphire templates. In situ XRD RSM measurements were performed using an MBE apparatus directly coupled to an X-ray diffractometer at the beamline of the synchrotron radiation facility SPring-8. It was observed in situ that both lattice relaxation and compositional pulling occurred during the initial growth stage, reducing the strain of GaInN on GaN and InN. Different initial growth behaviors of GaInN on GaN and InN were also observed from the results of the evolution of GaInN integrated peak intensities.

Keywords: GaInN; InGaN; MBE; in situ XRD RSM; heteroepitaxial growth

1. Introduction

Nitride-based red light-emitting diodes (LEDs) have been desired for the fabrication of nitride-based monolithic μ -LED displays providing the three primary colors of light. [1] Nitride-based red laser diodes (LDs) have also been desired to improve the poor temperature characteristics of AlGaInP-based LDs in order to fabricate laser displays [2].

In current nitride-based light emitters involving LEDs and LDs, a GaN-based matrix structure with GaInN quantum wells (QWs) has been used. With increasing the In content of GaInN in QWs in this structure, however, the increase in the spatial separation between electrons and holes and the plastic relaxation become serious problems that cannot be ignored. The former is owing to the enhancement of the quantum-confined Stark effect (QCSE) [3] due to a higher piezoelectric polarization. The latter is caused by the large lattice mismatch. On the other hand, a $\text{Ga}_x\text{In}_{1-x}\text{N}$ -based matrix structure with $\text{Ga}_y\text{In}_{1-y}\text{N}$ QWs ($x < y$) is expected to suppress the spatial separation between electrons and holes and the plastic relaxation in QWs.

Molecular beam epitaxy (MBE) has a major advantage for the growth of GaInN, especially for that with a high In content of over 20%, as it enables low-temperature growth compared with metal-organic chemical vapor deposition (MOCVD) and halide vapor deposition (HVPE). The growth of GaInN by MBE has been widely studied [4–11]. Owing to the elucidation of the optimum growth conditions [12]

and the development of growth technology such as metal-modulated epitaxy (MME) [13,14] and droplet elimination radical beam epitaxy (DERI) [15,16], the crystal quality of GaInN films has been improved.

However, serious problems still exist. For example, GaInN films must be grown on foreign substrates such as GaN/sapphire templates because of the lack of GaInN bulk substrates. Hence, when attempting to obtain high-quality GaInN templates grown on foreign substrates from the view point of configuring a GaInN matrix, it is important to know how to control strain relaxation and how to reduce the number of crystal defects generated by strain relaxation. GaInN films epitaxially grown on foreign substrates by MBE have been evaluated using ex situ X-ray diffraction and transmission electron microscopy (TEM) [12,17–22] in addition to in situ reflection high-energy electron diffraction (RHEED) measurements [4,20]. A few papers are available on the MOCVD growth of GaInN studied using in situ XRD [23,24] and X-ray reflectivity [25].

The strain state in a $\text{Ga}_x\text{In}_{1-x}\text{N}$ -based matrix structure is induced in the growth of not only $\text{Ga}_x\text{In}_{1-x}\text{N}$ on a foreign substrate but also $\text{Ga}_y\text{In}_{1-y}\text{N}$ on $\text{Ga}_x\text{In}_{1-x}\text{N}$ (under compressive strain) and $\text{Ga}_x\text{In}_{1-x}\text{N}$ on $\text{Ga}_y\text{In}_{1-y}\text{N}$ (under tensile strain) in QWs. Understanding of the growth mechanisms including strain relaxation is essential owing to the large lattice mismatch in a GaInN system which includes binary materials of GaN and InN.

In this study, in situ synchrotron XRD reciprocal space mapping (RSM) measurements were carried out for the radio-frequency plasma-assisted MBE (RF-MBE) growth of GaInN on GaN and InN.

2. Experimental Procedure

In situ XRD RSM measurements were performed using the MBE apparatus directly coupled to an X-ray diffractometer (Kohzu Precision Co., Ltd., Kawasaki, Japan) at beamline BL11XU of the synchrotron radiation facility SPring-8 (Hyogo, Japan) [26–28]. GaInN films were grown on GaN and InN. Commercialized HVPE-grown (0001)GaN templates with a thickness of 4.5 μm on *c*-sapphire templates (MTI corporation, Richmond, CA, USA) were used as substrates. Before the growth of GaInN, 15-nm-thick GaN layers were first grown at 650 °C to avoid the influence of the surface oxidation layer of the templates. In the case of GaInN growth on InN, a 15-nm-thick InN layer was additionally grown at 450 °C on the MBE-grown GaN layers. Of note is that this InN layer was completely relaxed from GaN. Then, GaInN films were grown both on GaN and InN layers at the same temperature of 450 °C, which is low enough to be able to ignore the thermal decomposition of InN during the growth of GaInN. The V/III ratio during the growth of GaInN was set to be less than 1 (a metal-rich condition). The solid In content of GaInN expected from the flux ratio between Ga and nitrogen radicals (N^*) [16] was about 55%. It is additionally worth noting that only In was supplied to the surface before the growth of GaInN. This amount of In was sufficient to cover the surface with a thickness of more than 2 monolayers (MLs), ensuring a metal-rich growth condition even in the first growth layer [16]. The nominal growth rate of GaInN was approximately 0.08 ML/s, which was estimated from the flux of N^* .

The energy of the incident X-rays was 20 keV and the beam size was 0.1 mm \times 0.1 mm. The diffracted X-ray signals from the samples were collected by a two-dimensional X-ray detector (PILATUS 100K) (DECTRIS Ltd., Baden, Switzerland). The two-dimensional (H [10–10] – L [0001] coordinate in Miller indices) RSM around the 10–11 diffraction peak was measured by adjusting the sample orientation and the detector position. An RSM image was taken every 7 s, that is, GaInN with a thickness of less than 1 ML was grown in one scan.

3. Results and Discussion

Figure 1 shows the RSMs during the growth of GaInN on GaN and InN taken after growth times of 98 s, 301 s, and 602 s as examples. The peak position was determined using a two-dimensional Gaussian fit. Figure 2 shows the evolution of the position of the 10–11 diffraction peak of the GaInN layer during the growth on GaN and InN. When the growth started, GaInN diffraction patterns extending in the L-coordinate direction appeared, as can be seen in Figure 1a,d. On GaN, the diffraction pattern was

confirmed to have a clear peak after the growth for approximately 140 s. After the appearance of the GaInN peak, the peak positions on both H and L were shifted in a direction away from the peak position of GaN. After growth for 300–500 s, the diffraction position on H was shifted further away from the GaN peak position, while that on L was conversely shifted toward the GaN peak position. On InN, the diffraction pattern was confirmed to show a clear peak after growth for approximately 160 s. After the appearance of the GaInN peak, the peak positions on both H and L were shifted in a direction away from the peak position of InN. After growth for 200–400 s, the diffraction position on H was shifted further away from the InN peak position, while that on L was conversely shifted toward the GaN peak position. These results indicate that both the In content and the relaxation ratio of GaInN were continuously changing during growth.

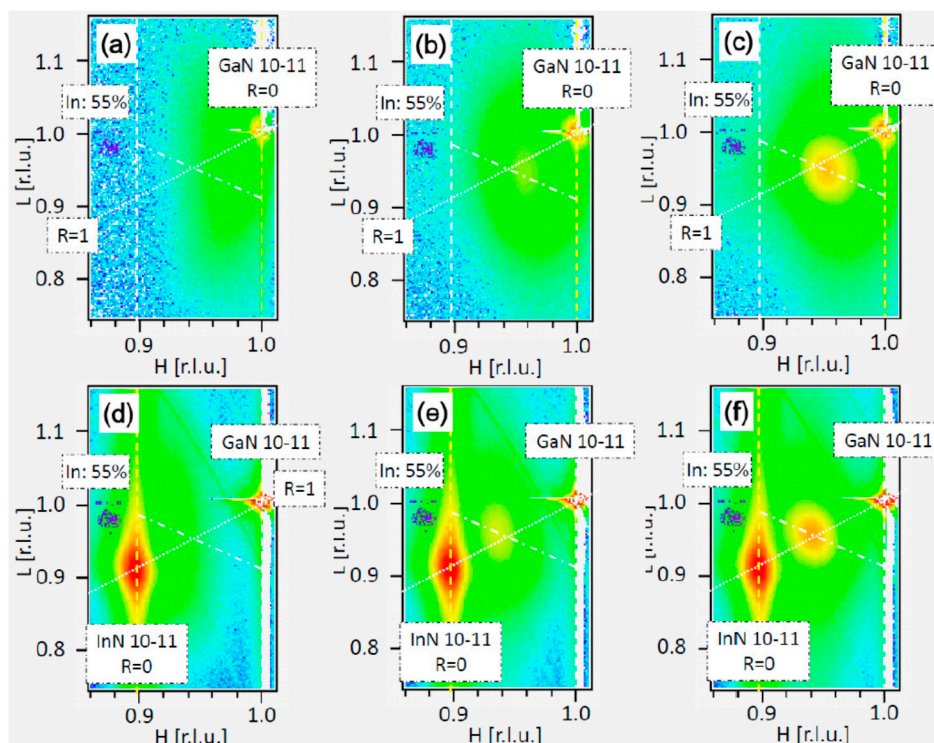


Figure 1. Reciprocal space mappings (RSMs) during growth on (a–c) GaN and (d–f) InN taken after growth times of (a,d) 98 s, (b,e) 301 s, and (c,f) 602 s. In these figures, r.l.u. indicates reciprocal lattice units.

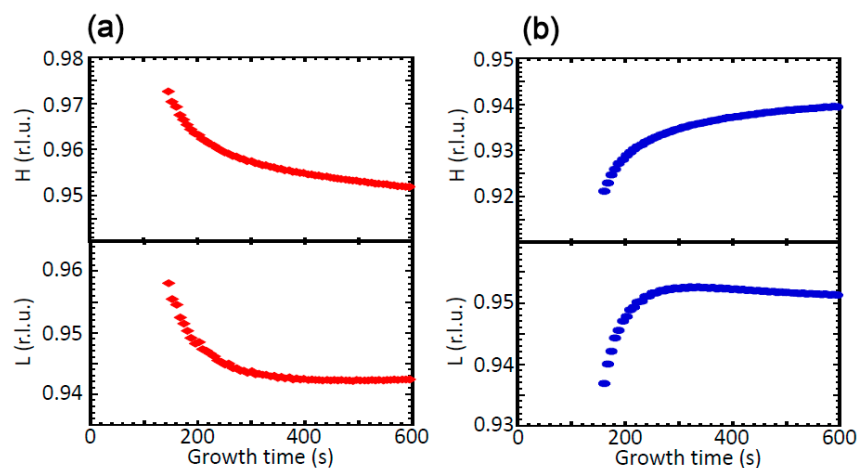


Figure 2. Evolution of position of 10–11 diffraction peak of GaInN layer during growth on (a) GaN and (b) InN.

The In content and relaxation ratio were estimated from the peak position of GaInN shown in Figure 2. Under biaxial stress, the relationship between the lattice constants along the c -axis and a -axis [17] is represented by

$$\frac{c_{(\text{GaInN})} - c_{0(\text{GaInN})}}{c_{0(\text{GaInN})}} = -2 \frac{c_{13}}{c_{33}} \cdot \frac{a_{(\text{GaInN})} - a_{0(\text{GaInN})}}{a_{0(\text{GaInN})}} \quad (1)$$

Here, c and a are the measured lattice parameters obtained from RSMs, c_0 and a_0 are the calculated lattice constants, and c_{13} and c_{33} are the elastic constants. The relaxation ratios of GaInN on GaN and on InN are respectively defined as

$$R_{\text{GaInN/GaN}} = \frac{a_{(\text{GaInN})} - a_{\text{GaN}}}{a_{0(\text{GaInN})} - a_{\text{GaN}}} \quad (2)$$

$$R_{\text{GaInN/InN}} = \frac{a_{(\text{InN})} - a_{(\text{GaInN})}}{a_{(\text{InN})} - a_{0(\text{GaInN})}} \quad (3)$$

In both Equations (2) and (3), $R = 0$ and $R = 1$ indicate a fully strained state and a fully relaxed state, respectively. The calculation of the lattice and elastic constants of GaN and InN utilized the values shown in Table 1 [29–31], which are referred to as the values at the growth temperature of 450 °C. The calculated lattice and elastic constants of GaInN with different In contents are given by Vegard's law.

Table 1. Lattice and elastic constants of GaN and InN at a growth temperature of 450 °C used in the calculations in this study.

| Materials | a [Å] | c [Å] | c_{13} [GPa] | c_{33} [GPa] |
|-----------|------------|------------|----------------|----------------|
| GaN | 3.191 [29] | 5.188 [29] | 97 [30] | 381 [30] |
| InN | 3.540 [31] | 5.705 [31] | 90 [31] | 218 [31] |

Figure 3 shows the evolution of the In content and the relaxation ratio of GaInN during the growth on GaN and InN. From the evolution of the relaxation ratio (Figure 3c,d), GaInN was found to gradually relax during this initial growth stage in both GaN and InN. Regarding the evolution of the In content in Figure 3a,b, for the first 300–400 s of the growth of GaInN, the In content increased and decreased on GaN and InN, respectively. After that, the content was almost constant at about 55%, which was the value expected from the supplied ratio under our metal-rich growth condition. These results can be explained by the fact that not only lattice relaxation but also compositional pulling [17,20,32,33] took place at the initial growth stage as a means of reducing the strain of GaInN on GaN (under compressive strain) and InN (under tensile strain). The well-known compositional pulling, observed by ex situ XRD measurements using GaInN samples grown with different thicknesses on GaN [17,20], was clearly observed throughout this in situ measurement. This result in the growth on GaN was in good agreement with the previous research results [17,20]. The In incorporation into GaInN is restricted to match the lattice of GaN. The observation of compositional pulling in the GaInN growth on InN has been observed for the first time, as far as the authors know. In the case, the In incorporation into GaInN is enhanced to match the lattice of InN.

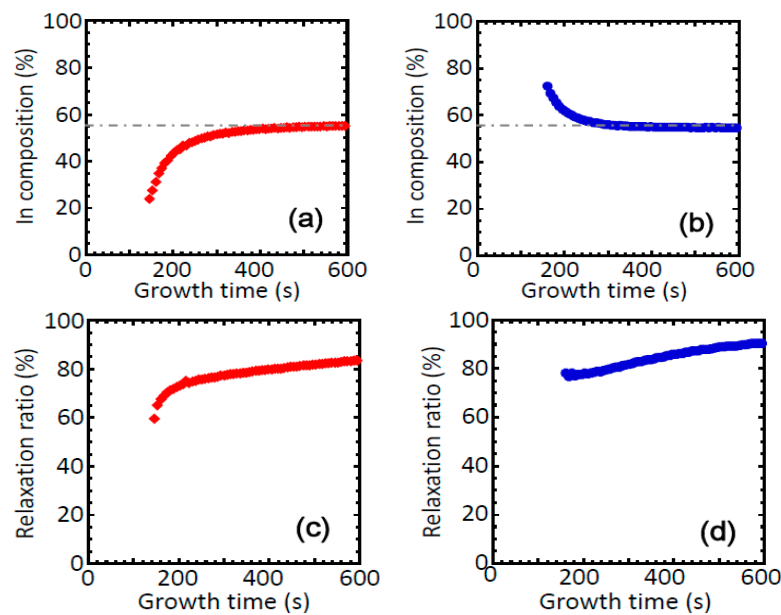


Figure 3. Evolution of (a,b) In composition and (c,d) relaxation ratio of GaInN during growth on (a,c) GaN and (b,d) InN.

Figure 4 shows the evolution of the integrated intensity of the GaInN 10–11 peaks during the growth on GaN and InN. A slow increase in the integrated intensity was observed in the initial growth stage on GaN. In the initial growth stage on InN, an almost constant increase in the integrated intensity was observed. Thus, different initial growth behaviors of GaInN on GaN and InN were observed. It can be concluded from these results that the growth rates on GaN and InN are different in the initial growth stage, since the slope of the change in the integrated intensity of the GaInN diffraction peak is related to the growth rate. The different transitions of the growth rate in the initial growth stage may be related to the different nucleation mechanisms, which are affected by factors such as surface stress, surface reconstruction, and surface instability of InN (e.g., interdiffusion into InN). During GaInN growth on InN under this condition, the integrated intensity of the InN 10-11 peak is almost constant. This means that the bulk InN underlayer is stable during the growth of GaInN. Although the surface instability of InN may affect to the nucleation of GaInN in the initial growth stage, the compositional gradient due to compositional pulling, which is appeared at the first 300 s of the growth of GaInN shown in Figure 3b, can be discussed independently. The detailed mechanism underlying the difference in the initial growth rate on GaN and InN is still under discussion. In order to discuss these strain relaxation processes quantitatively based on the conventional kinetic model [34], additional parameters regarding the pulling effect and nucleation process would be needed to be taken into account.

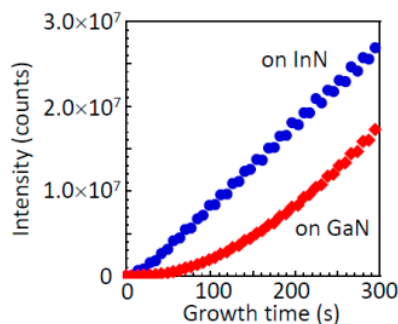


Figure 4. Evolution of integrated intensity of GaInN peaks during growth on GaN and InN.

4. Conclusions

In this work, the initial growth stages in the RF-MBE growth of GaInN on GaN and InN were observed using in situ synchrotron XRD RSM. It was observed in situ that both lattice relaxation and compositional pulling occurred during the initial growth stage, reducing the strain of GaInN on GaN and InN. Different initial growth behavior of GaInN on GaN and InN were also observed. These phenomena should also occur in the cases of high-In-content GaInN on low-In-content GaInN and low-In-content GaInN on high-In-content GaInN. The development of growth technology to control lattice relaxation, compositional pulling, and gradual change in the growth rate in the initial heteroepitaxial growth stage, as observed in this study, is necessary to fabricate high-quality GaInN matrix structures comprising a GaInN template and GaInN/GaN QWs.

Author Contributions: T.Y. conceived the idea of experiments. T.Y., T.S. and S.F. performed experiments. T.Y., T.S., M.T. and Y.N. analyzed the data. T.Y., T.S., S.F., M.T., T.A., T.O., T.H. and Y.N. discussed the results. T.Y. wrote the manuscript. T.Y., T.S., S.F., M.T., T.A., T.O., T.H. and Y.N. reviewed and edited the manuscript. T.Y., T.S. and M.T. acquired the funding.

Funding: This work was also partly supported by JSPS KAKENHI (grant numbers #17H02778, #19H05298, and #19H00874) and Kogakuin University Grant for the project research.

Acknowledgments: This work was partly supported by the MEXT Nanotechnology Platform, and the synchrotron radiation experiments were performed at BL11XU of SPring-8 (proposal nos. 2015A3512, 2016A3562, and 2017A3587).

Conflicts of Interest: The authors declare no conflict of interest.

References

1. Kishino, K.; Nagashima, K.; Yamano, K. Monolithic Integration of InGaN-Based Nanocolumn Light-Emitting Diodes with Different Emission Colors. *Appl. Phys. Express* **2013**, *6*, 012101. [[CrossRef](#)]
2. Kawanishi, H. IR/R/G/B laser diodes for multi-wavelength applications. *Opt. Rev.* **2019**, *26*, 152. [[CrossRef](#)]
3. Takeuchi, T.; Sota, S.; Katsuragawa, M.; Komori, M.; Takeuchi, H.; Amano, H.; Akasaki, I. Quantum-Confined Stark Effect due to Piezoelectric Fields in GaInN Strained Quantum Wells. *JPN J. Appl. Phys.* **1997**, *36*, L382. [[CrossRef](#)]
4. Grandjean, N.; Massies, J. Real time control of $\text{In}_x\text{Ga}_{1-x}\text{N}$ molecular beam epitaxy growth. *Appl. Phys. Lett.* **1998**, *72*, 1078. [[CrossRef](#)]
5. Böttcher, T.; Einfeldt, S.; Kirchner, V.; Figge, S.; Heinke, H.; Hommel, D.; Selke, H.; Ryder, P.L. Incorporation of indium during molecular beam epitaxy of InGaN. *Appl. Phys. Lett.* **1998**, *73*, 3232. [[CrossRef](#)]
6. O'Steen, M.L.; Fedler, F.; Hauenstein, R.J. Effect of substrate temperature and V/III flux ratio on In incorporation for InGaN/GaN heterostructures grown by plasma-assisted molecular-beam epitaxy. *Appl. Phys. Lett.* **1999**, *75*, 2280. [[CrossRef](#)]
7. Adelman, C.; Langer, R.; Feuillet, G.; Daudin, B. Indium incorporation during the growth of InGaN by molecular-beam epitaxy studied by reflection high-energy electron diffraction intensity oscillations. *Appl. Phys. Lett.* **1999**, *75*, 3518. [[CrossRef](#)]
8. Storm, D.F. Incorporation kinetics of indium and gallium in indium gallium nitride: A phenomenological model. *J. Appl. Phys.* **2001**, *89*, 2452. [[CrossRef](#)]
9. Nanishi, Y.; Saito, Y.; Yamaguchi, T. RF-molecular beam epitaxy growth and properties of InN and related alloys. *JPN J. Appl. Phys.* **2003**, *42*, 2549. [[CrossRef](#)]
10. Liu, Y.; Xie, M.H.; Cao, Y.G.; Wu, H.S.; Tong, S.Y. A Study of $\text{In}_x\text{Ga}_{1-x}\text{N}$ Growth by reflection high-energy electron diffraction. *J. Appl. Phys.* **2005**, *97*, 023502. [[CrossRef](#)]
11. Iliopoulos, E.; Georgakilas, A.; Dimakis, E.; Adikimenakis, A.; Tsagaraki, K.; Androulidaki, M.; Pelekanos, N.T. InGaN(0001) alloys grown in the entire composition range by plasma assisted molecular beam epitaxy. *Phys. Status Solidi A* **2006**, *203*, 102. [[CrossRef](#)]
12. Papadomanolaki, E.; Bazioti, C.; Kazazis, S.A.; Androulidaki, M.; Dimitrakopoulos, G.P.; Iliopoulos, E.E. Molecular beam epitaxy of thick InGaN(0001) films: Effects of substrate temperature on structural and electronic properties. *J. Cryst. Growth* **2016**, *437*, 20. [[CrossRef](#)]

13. Moseley, M.; Billingsley, D.; Henderson, W.; Trybus, E.; Doolittle, W.A. Transient atomic behavior and surface kinetics of GaN. *J. Appl. Phys.* **2009**, *106*, 014905. [[CrossRef](#)]
14. Moseley, M.; Gunning, B.; Greenlee, J.; Lowder, J.; Namkoong, G.; Doolittle, W.A. Observation and control of the surface kinetics of InGaN for the elimination of phase separation. *J. Appl. Phys.* **2012**, *112*, 014909. [[CrossRef](#)]
15. Yamaguchi, T.; Nanishi, Y. Indium Droplet Elimination by Radical Beam Irradiation for Reproducible and High-Quality Growth of InN by RF Molecular Beam Epitaxy. *Appl. Phys. Express* **2009**, *2*, 051001. [[CrossRef](#)]
16. Yamaguchi, T.; Uematsu, N.; Araki, T.; Honda, T.; Yoon, E.; Nanishi, Y. Growth of thick InGaN films with entire alloy composition using droplet elimination by radical-beam irradiation. *J. Cryst. Growth* **2013**, *377*, 123. [[CrossRef](#)]
17. Pereira, S.; Correia, M.R.; Pereira, E.; O'Donnell, K.P.; Alves, E.; Sequeira, A.D.; Franco, N.; Watson, I.M.; Deatcher, C.J. Strain and composition distributions in wurtzite InGaN/GaN layers extracted from x-ray reciprocal space mapping. *Appl. Phys. Lett.* **2002**, *80*, 3913. [[CrossRef](#)]
18. Fischer, A.M.; Wei, Y.O.; Ponce, F.A.; Moseley, M.; Gunning, B.; Doolittle, W.A. Highly luminescent, high-indium-content InGaN film with uniform composition and full misfit-strain relaxation. *Appl. Phys. Lett.* **2013**, *103*, 131101. [[CrossRef](#)]
19. Jiao, W.; Kong, W.; Li, J.; Collar, K.; Kim, T.-H.; Brown, A.S. The relationship between depth-resolved composition and strain relaxation in InAlN and InGaN films grown by molecular beam epitaxy. *Appl. Phys. Lett.* **2013**, *103*, 162102.
20. Valdueza-Felip, S.; Bellet-Amalric, E.; Núñez-Cascajero, A.; Wang, Y.; Chauvat, M.-P.; Ruterana, P.; Pouget, S.; Lorenz, K.; Alves, E.; Monroy, E. High In-content InGaN layers synthesized by plasma-assisted molecular-beam epitaxy: Growth conditions, strain relaxation, and In incorporation kinetics. *J. Appl. Phys.* **2014**, *116*, 233504. [[CrossRef](#)]
21. Fabien, C.A.M.; Gunning, B.P.; Doolittle, W.A.; Fischer, A.M.; Wei, Y.O.; Xie, H.; Ponce, F.A. Low-temperature growth of InGaN films over the entire composition range by MBE. *J. Cryst. Growth* **2015**, *425*, 115. [[CrossRef](#)]
22. Bazioti, C.; Papadomanolaki, E.; Kehagias, T.; Walther, T.; Smalc-Koziorowska, J.; Pavlidou, E.; Komninou, P.; Karakostas, T.; Iliopoulos, E.; Dimitrakopoulos, G.P. Defects, strain relaxation, and compositional grading in high indium content InGaN epilayers grown by molecular beam epitaxy. *J. Appl. Phys.* **2015**, *118*, 155301. [[CrossRef](#)]
23. Richard, M.-I.; Highland, M.J.; Fister, T.T.; Munkholm, A.; Mei, J.; Streiffer, S.K.; Thompson, C.; Fuoss, P.H.; Stephenson, G.B. *In situ* synchrotron x-ray studies of strain and composition evolution during metal-organic chemical vapor deposition of InGaN. *Appl. Phys. Lett.* **2010**, *96*, 051911. [[CrossRef](#)]
24. Kachkanov, V.; Dolbnya, I.; O'Donnell, K.; Lorenz, K.; Pereira, S.; Watson, I.; Sadler, T.; Li, H.; Zubialevich, V.; Parbrook, P. Characterisation of III-nitride materials by synchrotron X-ray microdiffraction reciprocal space mapping. *Phys. Status Solidi C* **2013**, *10*, 481. [[CrossRef](#)]
25. Ju, G.; Fuchi, S.; Tabuchi, M.; Amano, H.; Takeda, Y. Continuous *in situ* X-ray reflectivity investigation on epitaxial growth of InGaN by metalorganic vapor phase epitaxy. *J. Cryst. Growth* **2014**, *407*, 68. [[CrossRef](#)]
26. Sasaki, T.; Ishikawa, F.; Yamaguchi, T.; Takahasi, M. Nitride-MBE system for *in situ* synchrotron X-ray measurements. *JPN. J. Appl. Phys.* **2016**, *55*, 05FB05. [[CrossRef](#)]
27. Takahasi, M. *In situ* synchrotron X-ray diffraction study on epitaxial-growth dynamics of III-V semiconductors. *JPN J. Appl. Phys.* **2018**, *57*, 050101. [[CrossRef](#)]
28. Sasaki, T.; Takahasi, M. Real-time structural analysis of InGaAs/InAs/GaAs(1 1 1)A interfaces by *in situ* synchrotron X-ray reciprocal space mapping. *J. Cryst. Growth* **2019**, *512*, 33. [[CrossRef](#)]
29. Reeber, R.R.; Wang, K. Lattice parameters and thermal expansion of GaN. *J. Mater. Res.* **2000**, *15*, 40. [[CrossRef](#)]
30. Reeber, R.R.; Wang, K. High Temperature Elastic Constant Prediction of Some Group III-nitrides. *MRS Internet J. Nitride Semicond. Res.* **2001**, *6*, 3. [[CrossRef](#)]
31. Wang, K.; Reeber, R.R. Thermal expansion and elastic properties of InN. *Appl. Phys. Lett.* **2001**, *79*, 1602. [[CrossRef](#)]
32. Hiramatsu, K.; Kawaguchi, Y.; Shimizu, M.; Sawaki, N.; Zheleva, T.; Davis, R.F.; Tsuda, H.; Taki, W.; Kuwano, N.; Oki, K. The Composition Pulling Effect in MOVPE Grown InGaN on GaN and AlGaIn and its TEM Characterization. *MRS Internet J. Nitride Semicond. Res.* **1997**, *2*, 6. [[CrossRef](#)]

33. Inatomi, Y.; Kangawa, Y.; Ito, T.; Suski, T.; Kumagai, Y.; Kakimoto, K.; Koukitu, A. Theoretical study of the composition pulling effect in InGaN metalorganic vapor-phase epitaxy growth. *JPN J. Appl. Phys.* **2017**, *56*, 078003. [[CrossRef](#)]
34. Dodson, B.; Tsao, J.Y. Relaxation of strained-layer semiconductor structures via plastic flow. *Appl. Phys. Lett.* **1987**, *51*, 1325. [[CrossRef](#)]



© 2019 by the authors. Licensee MDPI, Basel, Switzerland. This article is an open access article distributed under the terms and conditions of the Creative Commons Attribution (CC BY) license (<http://creativecommons.org/licenses/by/4.0/>).